FINAL REPORT

Grant Number: **DE-SC0004876**

Title of Award: **"Polarization-coupled tunable resistive behavior in oxide ferroelectric heterostructures" (PI: Alexei Gruverman, Co-PIs: Evgeny Tsymbal, Chang-Beom Eom)**

Date of report covered: 09/01/10 – 01/31/17

Brief description of the main accomplishments:

1. Chemical Interface Engineering for Control of Polarization Imprint in $BaTiO_3$ Films

Surface-adsorbed polar molecules can significantly alter the ferroelectric properties of oxide thin films. To achieve fundamental understanding of the effect of surface adsorbates on the functional properties of the ferroelectric tunnel junctions, we investigated the effect of chemically-induced surface polarization pinning in the top few atomic layers of the water-exposed $BaTiO_3$ (BTO) films with $SrRuO_3$ (SRO) bottom electrodes on their imprint behavior. We find that the chemically-induced surface polarization is not switchable but reduces the polarization imprint and improves the bistability of ferroelectric phase in BTO tunnel junctions (Fig. 1).

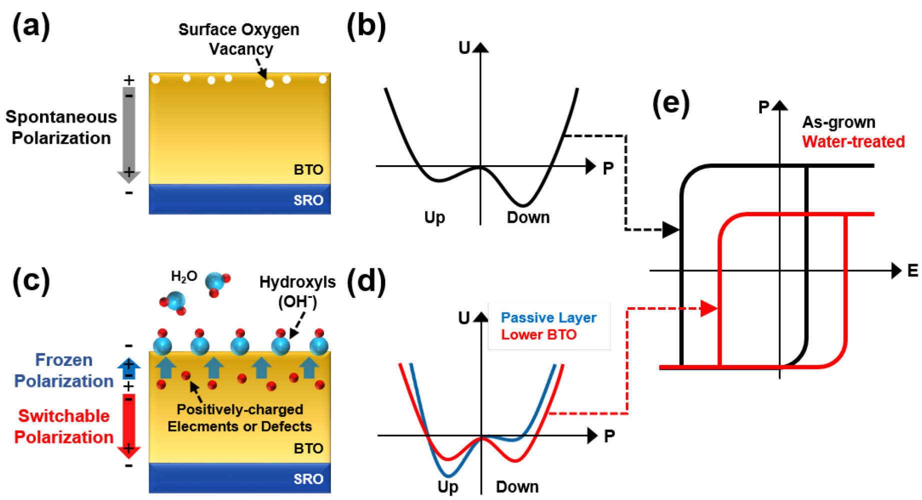

Figure 1. *(a) Schematics depicting the spontaneous polarization in a BTO thin film. Positive (negative) polarization charges are effectively screened by the electrons of SRO (surface oxygen vacancies), thereby stabilizing the downward polarization. (b) Energy diagram showing the asymmetric polarization states due to built-in potential in the BTO thin film. (c) Schematics depicting the chemically-induced polarization pinning effect in the BTO film. In the top passive layer, the positive (negative) polarization charges can be screened by hydroxyls (positively-charged defects). In the lower BTO region, the positive (negative) polarization charges can be screened by the electrons of SRO (positively-charged defects). (d) Energy diagram for the water-treated BTO thin film. Polarization states in the*

lower BTO thin film is symmetric, while that in the top passive layer is strongly asymmetric. (e) Expected shape of hysteresis loops of BTO thin film before and after the water treatment.

When a BTO thin film was exposed to water, the 2~3 top unit cells of the BTO formed a passive layer with polarization pinned at an upward orientation. The chemically-induced structural changes were studied by XRD. As a proof of concept, we fabricated FTJ structures using the water-treated BTO thin film. The water-treated samples exhibited symmetric hysteresis behavior, a smaller polarization imprint, and bistable equivalent polarization states, all of which are advantageous for device applications. This result can pave the way to a chemical approach for controlling the properties of ferroelectric thin films, enabling practical applications. We conclude that the chemical treatment of ferroelectric thin films with polar molecules may serve as a simple yet powerful strategy to enhance functional properties of ferroelectric tunnel junctions for their practical applications.

2. Electromechanics of Resistive Switching in $LaAlO_3/SrTiO_3$ Heterostructures

Recently, demonstration of tunable conductivity of the $LaAlO_3/SrTiO_3$ interfaces drew significant attention to the development of oxide electronic structures where electronic confinement can be reduced to the nanometer range. The highly conductive state at the interface between insulators $LaAlO_3$ and $SrTiO_3$ is a prime example of such emergent functionality, with potential application in high electron density transistors. In our studies, we have demonstrated a new paradigm for voltage-free tuning of $LaAlO_3/SrTiO_3$ interface conductivity, which involves the mechanical gating of interface conductance through stress exerted by the SPM tip. The mechanical control of channel conductivity and the long retention time of the induced resistance states enable transistor functionality with zero gate voltage.

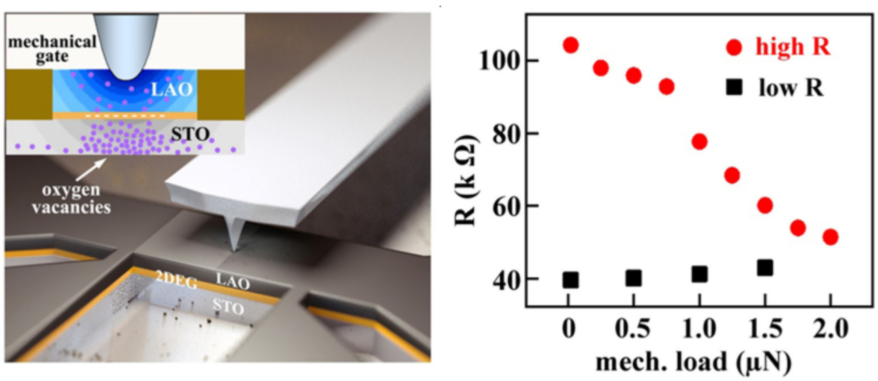

Figure 2. *Voltage-free tuning of the conductivity of the $LaAlO_3/SrTiO_3$ interface. This functionality is realized via the mechanical gating of interface resistance through mechanical stress, exerted by the tip of a scanning probe microscope (left panel). The continuous tunability of the mechanically-induced interfacial conductivity of the high-resistance state (right panel) enables electronic transistor devices with zero gate voltage.*

In parallel with these investigations of the $LaAlO_3/SrTiO_3$ interfaces, the physical properties of the $LaAlO_3$ layer itself have also been studied, and an unexpected FE-like behavior has been reported. We have investigated electrically and mechanically induced FE-like polar states of the $LaAlO_3$ thin films using a combination of scanning probe microscopy (SPM) techniques (Fig. 2). Analysis of the field-time dependent local polarization dynamics along with the transport measurements suggests that the FE-like behavior of the $LaAlO_3$ films is likely to arise from ion migration. We have proposed that this mechanism is associated with the reorganization of oxygen vacancies between the two stable states, which can be controlled at the sub-millisecond timescale using either the electrical or mechanical stimulus. These results indicate an importance of further studies of the role of ion dynamics in the resistive switching behavior in oxide heterostructures/interfaces and open new opportunities for control of the electronic properties at the nanoscale via a combined electro-mechanical approach.

3. ***Effect of Epitaxial Strain on Electroresistance Effect in Ferroelectric Tunnel Junctions***

During the reporting period, the IRG2 researchers were able to demonstrate their capability in performing synergetic research activities from the synthesis of high-quality epitaxial ferroelectric films, studying their transport characteristics and modeling their properties. The main focus was to experimentally study the parameters critical for tunneling electroresistance effect (TER) in FTJs. Specifically, we investigated the impact of epitaxial strain on the resistive behavior of the FTJs by testing the epitaxial $BaTiO_3/SrRuO_3$ bilayers fabricated on $SrTiO_3$ and $NdGaO_3$ substrates, which have different lattice mismatch with the ferroelectric barrier layer. A multi-target pulsed laser deposition (PLD) system equipped with a KrF excimer laser (λ = 248 nm) was used to grow the heterostructures. The thickness of the BTO films was controlled by monitoring the intensity oscillations of RHEED specular reflection. The crystal structure and thickness of the samples were analyzed using X-ray diffraction and X-ray reflectivity techniques. Piezoresponse force microscopy (PFM) was used for testing of the polarization state in the $BaTiO_3$ layers. The local I-V characteristics were measured using a conducting AFM (C-AFM) technique. Results of our studies showed that although the ferroelectric polarization of $BaTiO_3$ is presumably enhanced when the $BaTiO_3/SrRuO_3$ heterostructure is grown on the $NdGaO_3$ substrate due to a larger compressive strain, the TER effect is reduced (Fig. 3). We attribute this phenomenon to the strain-induced changes in the electronic properties of the $SrRuO_3$ films. Specifically, we suggest that the reduced TER in $BaTiO_3/SrRuO_3/NdGaO_3$ is due to the enhanced metallicity of $SrRuO_3$, grown on $NdGaO_3$, which reduces asymmetry of the potential profile in this heterostructures. Thus, a combined effect of strain on the ferroelectric polarization of the barrier and the screening properties of the electrodes needs to be taken into account when considering/predicting the TER effect in FTJs.

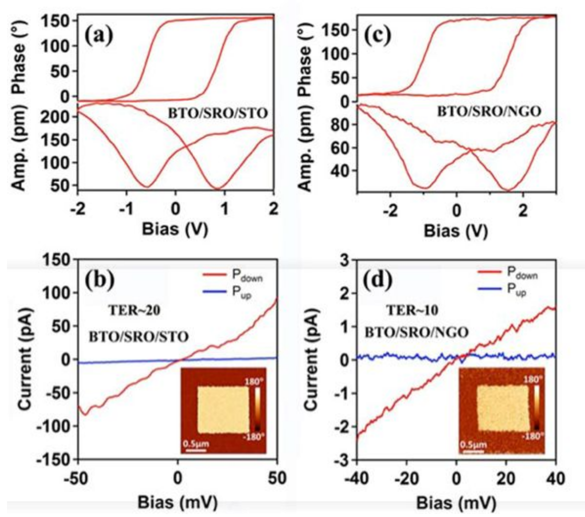

Figure 3. *Results of PFM and C-AFM testing of the 2.4-nm-thick $BaTiO_3$-based FTJs grown on (a,b) $SrRuO_3/SrTiO_3$ and (c,d) $SrRuO_3/NdGaO_3$ substrates. (a,c) PFM hysteresis loops and (b,d) I-V curves obtained in the FTJs poled downward with +3 V (red curves) and upward with -3 V (blue curves). Insets in (b,d) show PFM phase images of the $BaTiO_3$ films after poling with -3 V (lighter regions) and +3 V (darker regions).*

4. *Ferroelectric Tunnel Junctions with Graphene Electrodes*

During this project, we realized interface engineering through the introduction of molecular layers (MLs) at the interface between the ferroelectric layer and graphene, which is used as a top electrode of an FTJ. A molecular layer forms during the transfer of graphene to the ferroelectric surface in different solvents. Specifically, we have incorporated NH_3 layers at the graphene/$BaTiO_3$ interfaces. Introduction of the ammonia at the graphene/$BaTiO_3$ interface was achieved by washing the PMMA/graphene film with ammonium hydroxide solution (NH_3 sample) followed by its transfer to the $BaTiO_3$ surface after which the PMMA layer was removed by acetone. We denote junctions with graphene patches transferred in ammonia as Gr/NH_3/BTO junctions.

We characterized the resistive switching behavior by measuring the current-voltage (I-V) characteristics of the FTJs as a function of their polarization state using the conductive AFM (C-AFM) approach. Figure 4(a) shows the I-V curves measured after complete switching of the $BaTiO_3$ polarization either up or down by applying the +/-4 V voltage pulses. It is seen that there is a giant resistance change upon polarization reversal: the OFF/ON ratio R_{OFF}/R_{ON} reaches a factor of more than 3300 in the zero-bias limit and can be as large as 6000 for the bias range of ±0.2 V (Fig 4(b)). This effect is much stronger than that reported earlier for bare $BaTiO_3$ films of the same thickness (6 u.c.) with the TER magnitude of about 7. The observed effect is highly reproducible and stable: the I-V curves measured at different locations on the surface of the graphene patch display similar behavior and show no degradation with time within the period of polarization stability. In addition, C-AFM measurements performed on several different samples show little junction-to-junction variations. The obtained results suggest that the electrode/ferroelectric interface properties play a crucial role in the polarization-induced resistive switching behavior in FTJs. Introduction of the NH_3 layer at the graphene/$BaTiO_3$ interface not only stabilizes the polarization of $BaTiO_3$ but also significantly enhances the TER effect.

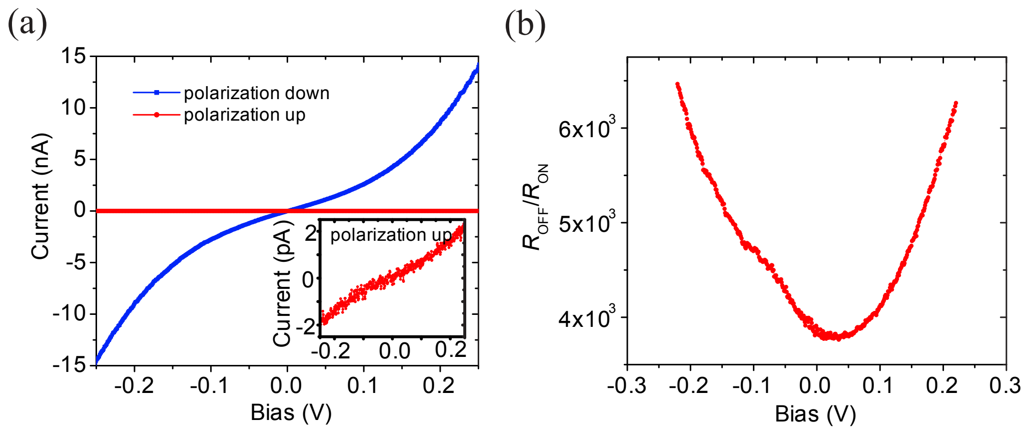

Figure 4. *Electroresistance effect in the Gr/NH_3/BTO/LSMO junctions. (a) The I-V curves measured for the upward (red) and downward (blue) $BaTiO_3$ polarization states. The inset shows the rescaled I-V curve for the upward polarization state. (b) R_{OFF}/R_{ON} resistance ratio as a function of the reading bias showing an increase up to 6000 for ±0.2 V. PFM testing of polarization after I-V measurements shows that polarization is not affected by the I-V measurements.*

5. *Ferroelectricity in Hexagonal $TbMnO_3$*

To support our experimental studies that revealed a room temperature ferroelectricity in epitaxially stabilized hexagonal $TbMnO_3$ (*h*-$TbMnO_3$) we have performed first-principles modelling of this material. We found that the ferroelectric non-centrosymmetric $P6_3cm$ phase of *h*-$TbMnO_3$ is energetically more favorable than the paraelectric centrosymmetric $P6_3/mmc$ phase with an energy difference of $\Delta E > 20$ meV/atom, which corresponds to ~1160 K/formula unit. Given that Curie temperature scales with ΔE, it can be expected that the T_C of *h*-$TbMnO_3$ is similar to that of *h*-$YMnO_3$ (1270 K). Berry phase calculations of the ferroelectric phase reveal that the spontaneous polarization is ~8 μC/cm^2 in the strain-free phase and ~18 μC/cm^2 in the strained phase, which is two orders of magnitude larger than the experimentally measured polarization of *o*-$TbMnO_3$ crystals at low temperature and comparable to the reported values of other *h*-*Re*MnO_3 single crystals, such as *h*-$YMnO_3$ (~5.5 μC/cm^2) and *h*-$HoMnO_3$ (~5.6 μC/cm^2).

6. *Mechanically-induced Electroresistance Effect in $BaTiO_3$ Films*

The mechanically-induced nonvolatile electroresistance effect in $BaTiO_3$ films facilitated by the flexoelectric switching of ferroelectric polarization resulting from application of local mechanical stress via an SPM tip has been previously demonstrated. It was found, that the tip-generated strain gradient in the film can produce a flexoelectric field that is strong enough to switch polarization in a way similar to an electric field (Figs 5(a,b)). Electrostatic force microscopy (EFM) images (Fig 5c) show a clear disparity between electrically and mechanically written domains: electrically produced domain indicates a higher screening charge density due to deposition of extra surface charge during switching. Figure 5d shows a current map obtained in the C-AFM mode where contrast variations correspond to changes in conductivity. It can be seen that both electrically and mechanically poled domains with downward polarization have higher conductivity in comparison to the as-grown $BaTiO_3$ film with upward polarization, which is indicative of the TER effect. It is interesting that the mechanically-induced TER is larger than the electrically-induced TER as is shown by local I-V measurements (Fig 5(e)): the resistance changes by 2300% for electrically poled domain versus 7300% resistance change for the mechanically written domain.

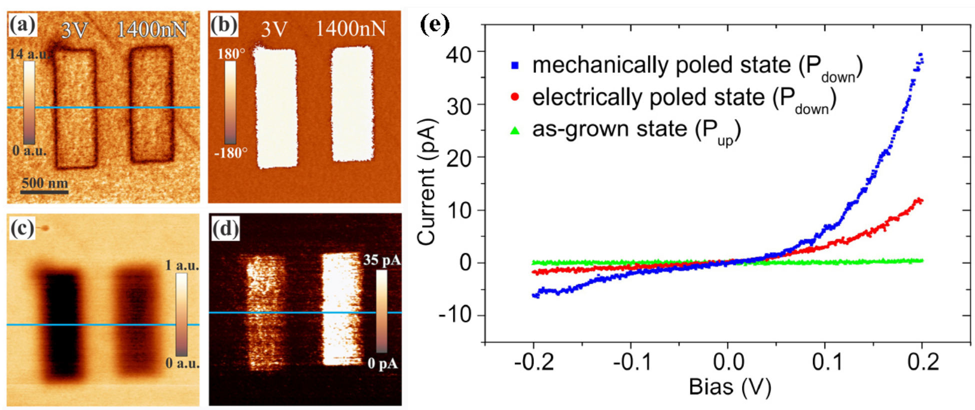

Figure 5. *SPM data illustrating the mechanically and electrically induced TER effects. (a, b) PFM amplitude (a) and phase (b) images of the 4-nm-thick* $BaTiO_3$ *film after domain writing by electrical poling (left) and mechanical loading (right). (c) EFM image of the same domains. (d) C-AFM current map at the same location. (e) I-V curves for mechanically and electrically written domains.*

A list of papers, where DOE support is acknowledged:

1. H. Lu, D. J. Kim, C. W. Bark, S. Ryu, C. B. Eom, E. Y. Tsymbal, and A. Gruverman, “Mechanically-Induced Tunneling Electroresistance Effect in Ultrathin Ferroelectrics”, Nano Lett. **12**, 6289-6292 (2012).

2. H. Lu, X. Liu, J. D. Burton, Y. Wang, Y. Zhang, D. J. Kim, A. Stamm, P. Lukashev, C. W. Bark, D. A. Felker, C. M. Folkman, P. Gao, X. Q. Pan, M. S. Rzchowski, C. B. Eom, E. Y. Tsymbal, and A. Gruverman, “Enhancement of Ferroelectric Polarization Stability by Interface Engineering”, Adv. Mat. **24**, 1209-1216 (2012).

3. H. Lu, C.W. Bark, D. Esque de los Ojos, J. Alcala, C.B. Eom, G. Catalan, and A. Gruverman, “Mechanical Writing of Ferroelectric Polarization”, Science **336**, 59-61 (2012).

4. D. J. Kim, H. Lu, S. Ryu, C. W. Bark, C. B. Eom, E. Y. Tsymbal, A. Gruverman, "Ferroelectric Tunnel Memristor", Nano Lett. **12**, 5697-5702 (2012).

5. C.W.Bark, P.Sharma, S.H.Beak, S.Lee, S.Ryu, C.M.Folkman, A.Kumar, S.V.Kalinin, E.Y.Tsymbal, M.S.Rzchowski, A.Gruverman, and C.B.Eom, “Switchable induced polarization in $LaAlO_3/SrTiO_3$ heterostructures”, Nano Lett. **12**, 1765-1771 (2012).

6. H. Lu, T. A. George, Y. Wang, I. Ketsman, J. D. Burton, C.-W. Bark, S. Ruy, D. J. Kim, J. Wang, C. Binek, P. A. Dowben, A. Sokolov, C.-B. Eom, E. Y. Tsymbal, and A. Gruverman, “Electric Modulation of Magnetization at Ferroelectric - Ferromagnetic Interfaces”, Appl. Phys Lett. **100**, 232904 (2012).

7. A.Stamm, D.J.Kim, H.Lu, C.W.Bark, C.B.Eom, and A.Gruverman, “Investigation of Polarization Relaxation Kinetics in Ultrathin Ferroelectric Capacitors”, Appl. Phys. Lett. **102**, 092901 (2013).

8. S. Cao, P. Liu, J. Tang, H. Lu, C. W. Bark, S. Ryu, C. B. Eom, A. Gruverman, and P. A. Dowben, “Magnetoelectric coupling at the $EuO/BaTiO_3$ interface”, Appl. Phys. Lett. **102**, 172402 (2013).

9. X. Liu, Y. Wang, J. D. Burton, and E. Y. Tsymbal, “Polarization controlled Ohmic to Schottky transition at a metal/ferroelectric interface,” *Physical Review B* **88**, 165139 (2013).

10. H. Lu, A. Lipatov, S. Ryu, D. J. Kim, M. Y. Zhuravlev, C. B. Eom, E. Y. Tsymbal, A. Sinitskii, and A. Gruverman, “Ferroelectric Tunnel Junctions with Graphene Electrodes: Critical Role of the Interfacial Layer”, Nat. Commun. **5**, 5518 (2014).

11. D.J.Kim, T.R.Paudel, H.Lu, J.D.Burton, J.G.Connell, E.Y.Tsymbal, S.S.A.Seo, and A.Gruverman, "Room-Temperature Ferroelectricity in Hexagonal $TbMnO_3$ thin films", Adv. Mat. **26**, 7660-7665 (2014). DOI: 10.1002/adma.201403301

12. J. Chen, A. Gruverman, A. N. Morozovska, and N. Valanoor, ”Sub-Critical Field Domain Reversal in Epitaxial Ferroelectric Films”, J. Appl. Phys. **116**, 124109 (2014).

13. X. Liu, J. D. Burton, M. Y. Zhuravlev, and E. Y. Tsymbal, “Electric control of spin injection into a ferroelectric semiconductor,” Physical Review Letters **114**, 046601 (2015).

14. H.Lee, T.H.Kim, J.J.Patzner, H.Lu, J.Lee, H.Zhou, W.Chang, M.K.Mahanthappa, E.Y.Tsymbal, A.Gruverman, and C.B.Eom, “Imprint Control of $BaTiO_3$ Thin films via Chemically-induced Surface Polarization Pinning”, Nano Lett. **16**, 2400-2406 (2016).

15. P.Sharma, S.Ryu, J.D.Burton, T.R.Paudel, C.W.Bark, Z.Huang, Ariando, E.Y.Tsymbal, G.Catalan, C.B.Eom, and A.Gruverman, “Mechanical Tuning of $LaAlO_3/SrTiO_3$ Interface Conductivity”, Nano Lett. **15**, 3547-3551 (2015).

16. P.Sharma, S.Ryu, Z.Viskadourakis, T.R.Paudel, H.Lee, C.Panagopoulos, E.Y.Tsymbal, C.B.Eom, and A.Gruverman, “Electro-Mechanics of Ferroelectric-like Behavior of $LaAlO_3$ Thin Films”, Adv. Funct. Mat. **25**, 6538-6544 (2015).

17. A.Sokolov, O.Bak, H.Lu, S.Li, E.Y.Tsymbal and A.Gruverman, “Effect of epitaxial strain on tunneling electroresistance in ferroelectric tunnel junctions”, Nanotechnology **26**, 305202 (2015).

18. D.J.Kim, J.G.Connell, S.S.A.Seo, and A.Gruverman, “Domain wall conductivity in semiconducting hexagonal ferroelectric $TbMnO_3$ thin films”, Nanotechnology **27**, 155705 (2016).

19. J.Očenášek, H.Lu, C.W.Bark, C.B.Eom, J.Alcalá, G.Catalan, and A.Gruverman, “Nanomechanics of Flexoelectric Switching”, Phys. Rev B **92**, 035417 (2015).